PAPER • OPEN ACCESS

Controlling ultrafast currents by the nonlinear photogalvanic effect

New Journal of Physics
The open access journal at the forefront of physics

Deutsche Physikalische Gesellschaft DPG
IOP Institute of Physics

Published in partnership with: Deutsche Physikalische Gesellschaft and the Institute of Physics

PAPER

Controlling ultrafast currents by the nonlinear photogalvanic effect

Georg Wachter[1], Shunsuke A Sato[2], Isabella Floss[1], Christoph Lemell[1,5], Xiao-Min Tong[2,3], Kazuhiro Yabana[2,3] and Joachim Burgdörfer[1,4]

[1] Institute for Theoretical Physics, Vienna University of Technology, A-1040 Vienna, Austria
[2] Graduate School of Pure and Applied Sciences, University of Tsukuba, Tsukuba 305-8571, Japan
[3] Center for Computational Sciences, University of Tsukuba, Tsukuba 305-8577, Japan
[4] Institute of Nuclear Research of the Hungarian Academy of Sciences (ATOMKI), Debrecen H-4001, Hungary
[5] Author to whom any correspondence should be addressed.

E-mail: Lemell@concord.itp.tuwien.ac.at

Keywords: ultrafast current, photogalvanic effect, TDDFT, SiO_2

OPEN ACCESS

RECEIVED
21 July 2015

REVISED
6 November 2015

ACCEPTED FOR PUBLICATION
12 November 2015

PUBLISHED
21 December 2015

Abstract

We investigate the effect of broken inversion symmetry on the generation and control of ultrafast currents in a transparent dielectric (SiO_2) by strong femtosecond optical laser pulses. *Ab initio* simulations based on time-dependent density functional theory predict ultrafast direct currents that can be viewed as a nonlinear photogalvanic effect. Most surprisingly, the direction of the current undergoes a sudden reversal above a critical threshold value of laser intensity of about $I_c \sim 3 \times 10^{13}$ W cm^{-2}. We trace this switching to the transition from nonlinear polarisation currents to the tunnelling excitation regime. The latter is found to be sensitive to the relative orientation between laser polarisation and chemical bonds. We demonstrate control of the ultrafast currents by the time delay between two laser pulses. While two temporally separated laser pulses lead to currents along one direction their temporal overlap can reverse the current. We find the ultrafast current control by the nonlinear photogalvanic effect to be remarkably robust and insensitive to the laser-pulse shape and the carrier-envelope phase.

1. Introduction

In the last decade, ultrafast few-cycle laser pulses with well-defined carrier-envelope phase (CEP) have become available providing novel opportunities to explore the ultrafast and nonlinear response of matter to strong optical fields. The study of the induced electronic motion and of the highly nonlinear optical response have focussed on rare gas atoms [1], molecules [2], and, more recently, on nanostructures, surfaces, and bulk matter [3–5]. The driven electron dynamics can be monitored through optical signals [6–10] and through emitted electrons [11–16]. Very recently, Schiffrin *et al* [17] have demonstrated directed electron currents generated inside transparent dielectrics by carefully tailored laser pulses. In turn, the ultrafast response can characterise the impinging laser field [18]. Currently, avenues are explored to exploit such ultrafast modulation of electric currents for petahertz-scale signal processing [19] enabled by the short intrinsic time scale of the electron motion (∼1 fs), orders of magnitude faster than semiconductor electronics.

In this work, we explore a novel channel for the ultrafast electronic response that is unique to dielectrics with a non-centrosymmetric crystallographic structure: the generation of direct currents (dc) induced by strong optical laser pulses. Fully three-dimensional *ab-initio* simulations based on time-dependent density functional theory (TD-DFT) predict the generation of strongly nonlinear currents in α-quartz that are, in contrast to previously observed currents [17, 18], *independent* of the details of the laser pulse shape. The direction of the currents is found to be sensitive to the instantaneous laser intensity. Analysis of the spatio-temporal charge dynamics on the atomic length and time scales allows us to link this to the transition from nonlinear polarisation currents to directional tunnelling excitation, the latter being highly sensitive to the alignment between the laser polarisation and the chemical bonds in the crystal. We demonstrate that this transition may be investigated in a pump-probe setup leaving its marks as a change of the direction of the current as a function of the pump-probe delay.

2. Method

Theoretical exploration of ultrafast processes in solids faces the challenge to tackle the time-dependent many-body problem. TD-DFT has emerged as a versatile tool allowing for an *ab-initio* description of a variety of nonlinear and strong field processes [20–24] including in the solid state [9, 14, 16, 25–27]. Here, we employ a real-space, real-time formulation of TD-DFT [28–33] for the electronic dynamics induced by strong few-cycle laser pulses in α-SiO_2 (α-quartz). Briefly, we solve the time-dependent Kohn–Sham equations (atomic units are used unless stated otherwise)

$$\mathrm{i}\partial_t \psi_i(\mathbf{r}, t) = H(\mathbf{r}, t)\psi_i(\mathbf{r}, t), \tag{1}$$

where i runs over the occupied Kohn–Sham orbitals ψ_i. The Hamiltonian

$$H(\mathbf{r}, t) = \frac{1}{2}(-i\boldsymbol{\nabla} + \mathbf{A}(t))^2 + \hat{V}_{\mathrm{ir}} + \int \mathrm{d}\mathbf{r}' \frac{n(\mathbf{r}', t)}{|\mathbf{r} - \mathbf{r}'|} + \hat{V}_{\mathrm{XC}}(\mathbf{r}, t) \tag{2}$$

describes the system under the influence of a homogeneous time-dependent electric field $\mathbf{F}(t)$ of amplitude $\mathbf{F}_0$ along $\hat{a}$ with vector potential $\mathbf{A}(t) = -\int_{-\infty}^{t} \mathbf{F}(t')\mathrm{d}t'$ in the velocity gauge. The periodic lattice potential $\hat{V}_{\mathrm{ion}}$ is given by norm-conserving pseudopotentials of the Troullier–Martins form [34] representing the ionic cores ($O(1s^2)$ and $Si(1s^2 2s^2 2p^6)$). The valence electron density is $n(\mathbf{r}, t) = \sum_i |\psi_i(\mathbf{r}, t)|^2$. For the exchange and correlation potential $\hat{V}_{\mathrm{XC}}$ we employ the adiabatic Tran–Blaha modified Becke–Johnson (TB-mBJ) meta-GGA functional [35–37]. The validity of the adiabatic approximation is still an open question [38]. For example, representing driven few-state dynamics, in particular Rabi oscillations, by adiabatic functionals has been found to be difficult [39, 40]. However, implementation of functionals that include effects non-local in time [41] into realistic three-dimensional simulations have remained a challenge. Currently, the applicability of adiabatic functionals to ultrafast phenomena can only be assessed by comparison with experiment. Good agreement for a wide array of observables including high-harmonic generation [20], electronic dynamics in metal clusters [22] and semiconductors [9], as well as reflectance and ablation [27] point to its usefulness and approximate validity. One likely reason for its success is that for these cases of many-particle systems the coherent dynamics involves averaging over a large number of states. The TB-mBJ functional accurately reproduces the band gap $\Delta \sim 9$ eV for SiO_2 and yields good agreement with the experimental dielectric function over the spectral range of interest including at optical frequencies [42].

The time-dependent Kohn–Sham equations (1) are solved in the transverse geometry [43] to treat the bulk polarisation response of the infinitely extended system along the polarisation direction. We use a Cartesian grid with discretisation ~0.25 a.u. in laser polarisation direction and ~0.45 a.u. perpendicular to the polarisation direction in a cuboid cell of dimensions $9.28 \times 16.05 \times 10.21$ a.u.^{3} employing a nine-point stencil for the kinetic energy operator and a Bloch-momentum grid of $4^3\,\mathbf{k}$-points. The time evolution is performed with a 4th-order Taylor approximation to the Hamiltonian with a time step of 0.02 a.u. including a predictor-corrector step. The solution of equations (1) and (2) allows to analyze the time and space dependent microscopic vectorial current density

$$\mathbf{j}(\mathbf{r}, t) = \sum_i \frac{1}{2}\left[\psi_i^*(\mathbf{r}, t)(-\mathrm{i}\boldsymbol{\nabla} + \mathbf{A}(t))\psi_i(\mathbf{r}, t) + \mathrm{c.c.}\right] \tag{3}$$

as well as the mean current density $J(t)$ along the laser polarisation direction $\mathbf{F}_0$, averaged over the unit cell of volume Ω,

$$J(t) = \frac{1}{\Omega}\int_{\Omega} \mathrm{d}\mathbf{r}\, \mathbf{j}(\mathbf{r}, t) \cdot \mathbf{F}_0 / |F_0|. \tag{4}$$

The polarisation density $P(t) = \int_{-\infty}^{t} J(t')\mathrm{d}t'$ [44] gives the charge density $D(t)$ transferred by the pulse. The experimentally observed total charge Q will depend also on the details of the geometry of the laser focus and of the collection volume not explicitly treated in the following.

While dephasing due to elastic scattering is self-consistently included in TD-DFT, inelastic electron–phonon and electron–electron scattering is not. For low excitation densities and large band gap insulators electron-electron scattering can be neglected [45]. Electron–phonon scattering can be included on a phenomenological (i.e., non-self consistent) level via damping or relaxation rates. The possible influence of relaxation on the anisotropy of the induced nonlinear current are estimated by applying the quantum friction approach of Neuhauser and Lopata [46] and a purely phenomenological approach employing damping constants.

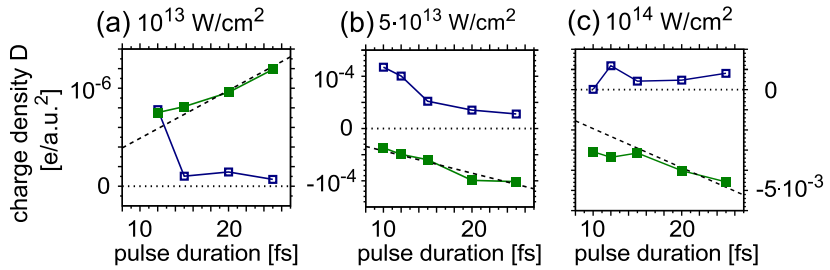

Figure 1. Pulse length dependence of transferred charge at intensities (a) 10^{13} W cm^{-2}, (b) 5×10^{13} W cm^{-2} and (c) 10^{14} W cm^{-2}, each with cos^2 pulse shape. Carrier-envelope phase dependent part D_{CEP} (blue open squares); CEP independent part D_0 (green full squares); dashed lines: linear slope going through the origin.

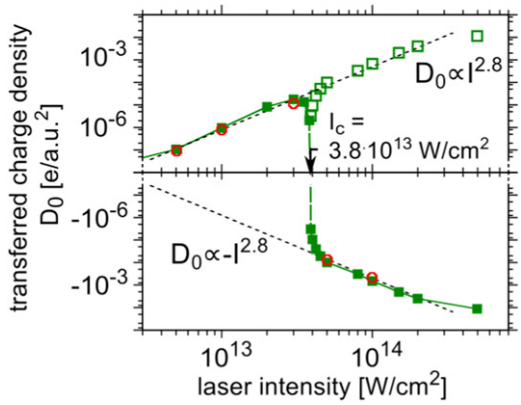

Figure 2. Carrier-envelope phase *independent* transferred charge density D_0 (green full squares) as function of laser intensity (cos^2 pulse with full duration $\tau_p = 20$ fs, $\hbar\omega_{\mathrm{L}} = 1.7$ eV) and absolute value $|D_0|$ (open squares). Red circles show the values of D_0 for selected laser intensities including strong damping ($\alpha = 10$ corresponding to a damping time of ~1 fs). Power law $|D_0| \propto I^{2.8}$ (dashed line). Electrons move along $+\hat{a}$ for $I \leqslant I_{\mathrm{c}} = 3.8 \times 10^{13}$ W cm^{-2} (upper panel) and along $-\hat{a}$ for $I \gtrsim I_{\mathrm{c}}$.

3. Nonlinear direct currents

First studies of the short-pulse induced current and charge transfer in polycrystalline SiO_2 [17, 18, 33] found a sinusoidal dependence on the CEP, ϕ_{CE}, of the few-cycle electromagnetic field $\mathbf{A}(t) \sim \mathbf{A}_0(t)\cos(\omega_{\mathrm{L}} t + \phi_{\mathrm{CE}})$ with cos^2-envelope $\mathbf{A}_0(t)$ and ω_{L} the carrier frequency of the IR laser. Sub-cycle control and steering of electrons required exquisite control over the instantaneous electric field $\mathbf{F}(t)$. The direction of the induced current was found to be determined by the CE phase and, thus, by the anisotropy of the few-cycle laser pulse. Here, we explore an alternate route towards steering, controlling and switching ultrafast currents that does not rely on ϕ_{CE} control of the instantaneous field but on the instantaneous intensity dependence of a (dc) that is applicable for longer laser pulses where CEP effects become negligible. We propose to exploit the non-inversion symmetric lattice structure of the target (in this case polarization parallel to the $\hat{a}$ direction of SiO_2) to cause an intensity dependence of the direction of the charge transfer which can be tested in a simple pump-probe setting described in section 4.

Starting point is the observation that the total charge density $D(\tau_p)$ transferred at the conclusion of the pulse can be split into a CEP dependent part with amplitude $D_{\mathrm{CEP}}(\tau_p)$ which vanishes upon averaging over ϕ_{CE} and a residual or direct part $D_0(\tau_p)$. $D_{\mathrm{CEP}}(\tau_p)$ tends to decrease with increasing pulse length while the magnitude of $D_0(\tau_p)$ increases with the pulse length (figure 1). For pulse lengths exceeding a few optical cycles ($\tau_p \gtrsim 15$ fs, $\lambda = 750$ nm), $D_0(\tau_p)$ is approximately proportional to the pulse duration and dominates the signal exceeding D_{CEP} by about one order of magnitude. The directionality of D_0 is the focus of the present investigation.

The charge transferred by the induced dc current, $D_0(\tau_p)$, features a strongly nonlinear scaling with intensity $|D_0| \propto I^{2.8}$ or, equivalently, field strength $|D_0| \propto F_0^{5.6}$ (figure 2). The origin of this highly nonlinear response lies in the broken centrosymmetry of the SiO_2 crystal along the $\hat{a}$ direction. In general, generation of a directed flow of charge by a laser field requires a broken inversion symmetry. For few-cycle laser pulses with well-defined CEP, inversion symmetry is violated by a suitable choice of ϕ_{CE}. In the present case, it is not the

temporal shape of the laser electric field but the electronic and crystallographic structure of the target the laser interacts with that causes ultrafast currents. This novel mechanism does not rely on delicate CEP control yet offers sub-cycle response and switching. The effect is also robust against damping and relaxation included into the simulations by adding a Drude-friction term

$$\dot{\mathbf{A}}_f(t) = -\mathbf{F}_f(t) = \alpha\,\mathbf{J}(t) \tag{5}$$

to the vector potential in equation (2) with damping constant α.

The appearance of a direct current in a homogeneous medium under illumination, independent of the CEP, and linearly increasing with pulse duration, can be viewed as a nonlinear analogue to the well-known photogalvanic (PG) effect [47–51] as first qualitatively discussed by Alon [52]. Conventionally, the lowest order photogalvanic effect is described by

$$J_k^{\mathrm{PG}} = \beta_{\mathrm{kln}} F_l F_n^*. \tag{6}$$

J^{PG} is quadratic in the electric field components and linear in the time-averaged laser intensity $I \propto F_l F_l^*$. For linearly polarized light, the photogalvanic tensor β_{kln} associated with the two-wave mixing in the second-order susceptibility $\chi^{(2)}_{\mathrm{kln}}(0;\,\omega,\,-\omega)$ is non-zero only in non-centrosymmetric crystals [53]. Microscopically, a variety of mechanisms may contribute to the PG effect such as asymmetric excitation, scattering, or recombination of electrons and electronic defects [48]. One important realisation is the so-called 'shift current' [53–55] due to the shift between the centre of charge of the valence electrons and the excited electrons in the conduction band. This shift current has been predicted to be important in several semi-conductors [53, 56, 57] and has been first experimentally verified for ferroelectrics [55].

The present nonlinear generalisation of the photogalvanic effects is obviously a signature of strong-field interaction with matter. This is underscored by the surprising observation of current reversal as a function of laser intensity (figure 2). We find a critical value of current reversal at $I_c \approx 3.8 \times 10^{13}\,\mathrm{W\,cm^{-2}}$. Electrons move preferentially along the $+\hat{a}$ direction for lower intensities $I \lesssim I_c$ while they propagate along $-\hat{a}$ direction for higher intensities $I \gtrsim I_c$. We have checked that this effect does not sensitively depend on the XC functional employed and is also obtained with the local density approximation [58]. We have also checked that the sign reversal persists when relaxation is included on a phenomenological level. We find the magnitude of the charge transfer to be somewhat reduced, its intensity dependence and, most notably, the sign inversion above a critical intensity I_c (figure 2) remain unchanged. We expect the sign reversal of the transferred charge to be experimentally observable.

We elucidate the microscopic mechanism for this reversal by analysis of the spatio-temporal charge dynamics. At lower intensities $I < I_c$, the multi-photon driven nonlinear polarisation current leads to a localized accumulation of charge in between the Si-O bonds as displayed in the time-averaged density fluctuations at the conclusion of the laser pulse (inset figure 3(e)). This implies the formation of an induced atomic-scale dipole around the oxygen atoms, i.e. a displacement of the centre of charge by vertical excitation, resembling the shift current mechanism of the standard photogalvanic effect but generalized to higher order reflected in the nonlinear intensity scaling of $|D_0| \sim I^{2.8}$. We have verified that for $I < I_c$ the direction of charge transfer agrees with that of the linear photogalvanic effect observed at lower intensities but higher photon energies. The nonlinear charge transfer along the $+\hat{a}$ direction can thus be viewed as the strong-field (or multi-photon) realisation of the shift current. For higher laser intensities $I > I_c$ the dominant charge transfer mechanism is excitation of the tilted conduction band by tunnelling. Tunnelling significantly depends on the local potential landscape in the tunnelling direction. We find tunnelling is enhanced when the bond direction is aligned with the laser field as illustrated by a strongly asymmetric current density at times near the maxima of the electric field (figures 3(c) and (d)). Excitations along the Si–O–Si bond chain give rise to a current after the conclusion of the laser pulse (figure 3(f)). Tunnelling excitation is more efficient along $-\hat{a}$ where the O–Si bond is more closely aligned with the laser field (bond-alignment angle $\gamma_1 = 25.3°$) while in $+\hat{a}$ direction tunnelling is suppressed because of the larger angle ($\gamma_2 = 51.5°$) between the bond axis and the laser polarisation (along $\hat{a}$). Following tunnelling excitation to the conduction band, the current is mainly driven along the helical channel formed by the O–Si–O–Si–O chain along the $\hat{a}$ direction (see labelled atoms in figure 3(c) and light contours in (d) and (e)). The reversal of the charge transfer and current direction is therefore most likely associated with the increased weight of tunnelling excitation, consistent with the onset of a sub-cycle time structure of charge transfer for $I > I_c$. The transition to tunnelling excitation is therefore accompanied by a reversal of the charge transfer and current direction. As tunnelling rates scale exponentially with the peak intensity $\propto \exp(-1/\sqrt{I})$, the transition is quite abrupt suggesting its potential for femtosecond current switching. It is worth noting that despite the sudden switch in direction the overall intensity dependence of the transferred charge density is comparatively smooth. This observation is in line with other strong-field phenomena such as ionization that also display a smooth dependence on peak-field intensity of ultrashort pulses when crossing from the multi-photon to the tunnelling regime (e.g., [59]).

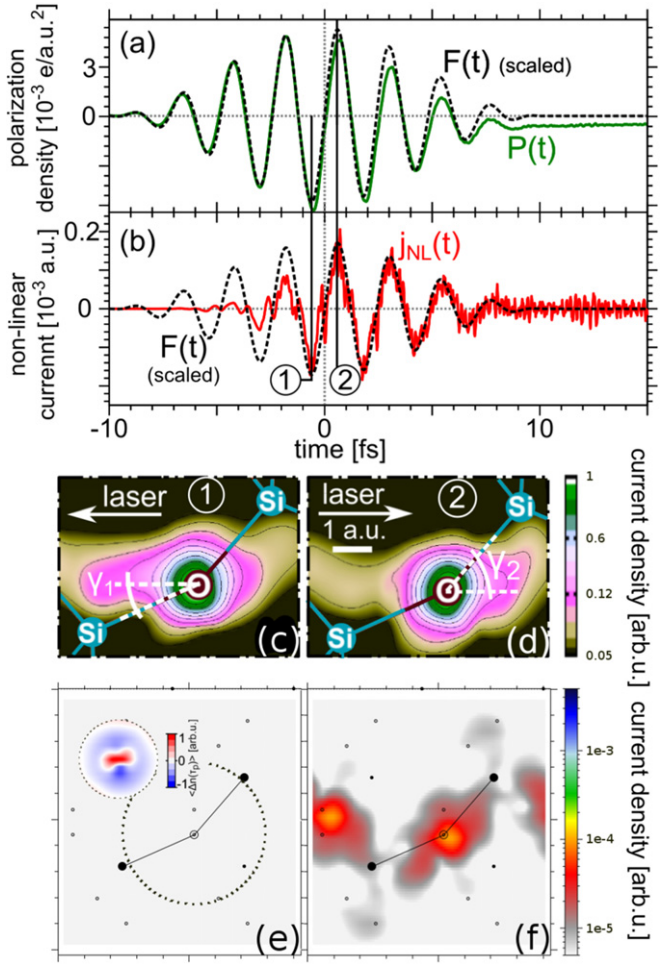

Figure 3. (a) Time-dependent polarisation density $P(t)$ (solid green), laser field $F(t)$ (black dashed, scaled) for $\tau_p = 20$ fs, $\hbar\omega_L = 1.7$ eV, intensity $I = 10^{14}$ W cm^{-2}. (b) Time-dependent nonlinear current ΔJ_{NL} (equation (7), red solid). (c), (d) Snapshot of the current density in an $\hat{a}$-$\hat{c}$ cut plane going through the central oxygen at a time ① (c), ② (d). Angles between the electric field and the O-Si bond are $\gamma_1 = 25.3°$, $\gamma_2 = 51.5°$. (e), (f) Current density after conclusion of the laser pulse for $I = 10^{13}$ W cm^{-2} (e) and $I = 10^{14}$ W cm^{-2} (f). While a current flows along the Si–O–Si bonds for $I = 10^{14}$ W cm^{-2}, we find no current for $I = 10^{13}$ W cm^{-2} on the same colour scale. (inset panel e) Time-averaged density modulation after the laser pulse $\Delta n(\tau_p)$ in plane cut through the central oxygen atom on a magnified colour scale.

4. Pump-probe protocol for dc currents

For all laser intensities, the dominant part of the CEP-independent dc charge transfer happens *during* the laser pulse (figure 3(a)), in contrast to the CEP-controlled ac charge transfer [33]. For high intensities $I > I_c$, the charge transfer shows sub-cycle time structure. The time-dependence of the tunnelling current can be conveniently analysed by the nonlinear response contribution $\Delta J_{NL}(t)$ after subtracting the linear-response current scaled to the instantaneous field,

$$\Delta J_{NL}(t) = J(t) - \frac{1}{2\pi}\int_{-\infty}^{\infty} e^{-i\omega t}\sigma(\omega)F(\omega) \tag{7}$$

with the conductivity $\sigma(\omega)$ determined for low intensity $I < I_c$ [43]. During the rise time of the pulse (figure 3(b)) ΔJ_{NL} is still ≈ 0 as linear response prevails. However, once a field strength sufficient for tunnelling between neighbouring atoms is reached around $t = -3$ fs, the nonlinear current shows strong spikes. While the linear response current is, to a good approximation, 90° out of phase with the electric field and the polarisation $P(t) = \int_{-\infty}^{t} dt' J(t')$ is in phase with $F(t)$, the current spikes are in phase with $F(t)$ as expected for tunnelling excitation. At later times (from $t = -1$ fs on), ΔJ_{NL} remains in phase with, and becomes proportional to the laser field, indicative of a conductor-like linear response $J(t) = \sigma_D F(t)$ with a Drude (free carrier-like) conductivity σ_D for the tunnelling-induced electron population in the conduction band.

The present analysis of the nonlinear photogalvanic dc current suggests that the key control parameter is the instantaneous intensity $I(t)$ rather than the cycle averaged intensity in the conventional photogalvanic effect or the instantaneous value of the field $F(t)$ in the CEP controlled ac current. This sensitivity to $I(t)$ can be explored in a

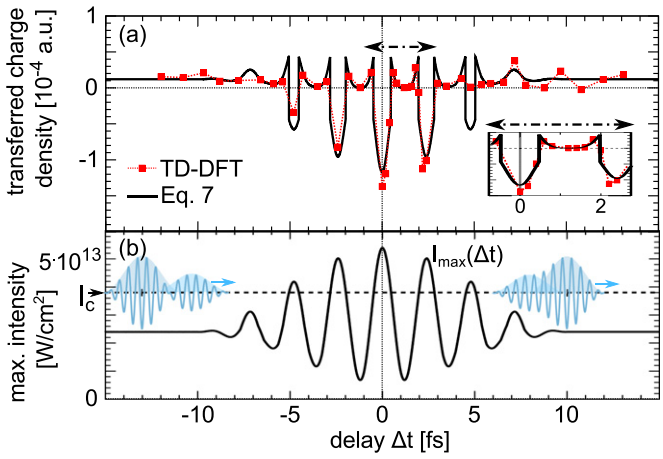

Figure 4. (a) Laser-induced transferred charge density as a function of the peak-peak delay ($I_1 = 2.4 \times 10^{13}$ W cm^{-2}, $I_2 = 0.6 \times 10^{13}$ W cm^{-2}, $\hbar\omega_L = 1.7$ eV, $\tau_p = 20$ fs). Red squares, dashed line: TD-DFT simulations; solid line: model equation (8). Inset: magnified data around $\Delta t \sim 0$ to 2 fs (dashed–dotted arrow). (b) Maximum instantaneous laser intensity $I(t) = F(t)^2(c/8\pi)$ for a given pump-probe delay. Insets: pulse shape after superposition of pump and probe pulse $F(t)$ at $\Delta t = -13$ fs (weak pulse before strong pulse) and at +10 fs.

pump–probe setting, in which the instantaneous intensity can by manipulated by the delay between pump and probe pulses. The pump–probe delay may therefore serve as knob for fast charge transfer by the nonlinear photogalvanic effect. To demonstrate this control we choose the intensity of both pump and probe pulses to be separately subcritical ($I_{1,2} < I_c$) with pump intensity $I_1 = 2.4 \times 10^{13}$ W cm^{-2} and probe intensity $I_2 = 0.6 \times 10^{13}$ W cm^{-2}. However, the superimposed fields give rise to a maximum intensity of $I_{max} = 2.25 I_1 = 5.4 \times 10^{13}$ W cm^{-2} above I_c. The sign and amplitude of the induced current is controlled by the time delay between the laser pulses (figure 4).

For large positive and negative delays, the transferred charge saturates at the same positive value. In contrast, for near-zero delay $\Delta t = 0$ where the maximum intensity is attained, the dc current switches direction and the transferred charge becomes negative. Remarkably, during the period of strong overlap the modulation of the dc current occurs on the sub-fs time scale resulting from the strongly varying maximum instantaneous laser intensity as a function of pump–probe delay (figure 4(b)).

Assuming that the charge transfer is governed by the central peak of the combined laser pulse, a simple estimate in analogy to equation (6) predicts

$$D(\Delta t) = \mathrm{sgn}\Big(I_c - I_{max}(\Delta t)\Big)\, \beta_{NL}\, I_{max}(\Delta t)^{2.8}, \tag{8}$$

where sgn denotes the sign function and $I_{max}(\Delta t)$ is the maximum instantaneous laser intensity for pump–probe delay Δt (figure 4(b)). In equation (8), we denote the nonlinear generalisation of the photogalvanic tensor by β_{NL}. This simple model reproduces the temporal variation of $D(\Delta t)$ in the full TD-DFT calculations remarkably well, underlining that the maximum instantaneous laser field drives the nonlinear photogalvanic effect through tunnelling near the field maximum.

5. Conclusions

We predict a nonlinear extension of the photogalvanic effect into the strong-field regime giving rise to ultrafast dc currents in insulators illuminated by multi-femtosecond laser pulses. We observe a strongly nonlinear intensity dependence and even a reversal of the induced currents above a critical intensity I_c associated with the transition from nonlinear polarisation currents to tunnelling excitation. The charge transfer is rather insensitive to details of the laser pulse shape and CEP but strongly dependent on the maximum instantaneous field strength. The latter may be controlled by the pump–probe delay in a two-pulse setup giving rise to a distinct sign change in the transferred charge as function of the pump–probe delay. The nonlinear photogalvanic effect opens up opportunities for light-field controlled femtosecond charge separation with relatively modest requirements on the driving laser. Even many-cycle pulses without CEP stabilisation can be used as the lattice structure instead of the CEP is employed to break the inversion symmetry along the laser polarisation axis. The nonlinear photogalvanic effect is conceptually simpler than the CEP dependent charge transfer since no elaborate steering of the conduction band electrons is necessary. Therefore, the effect is robust against changes in the laser pulse parameters. We envision the nonlinear photogalvanic effect may be useful for ultrafast signal processing as the

sign of the current may be controlled by the time delay between two laser pulses only, and does not rely on stable and custom-tailored wave shapes nor short pulses with only a few cycles. This may be advantageous in particular for optical interconnects based on surface plasmon propagation [19] where the pulse shape and duration of a surface plasmon wave packet are difficult to control. The relatively sharp threshold intensity I_c for reversal of the current may provide a simple route towards femtosecond current switching and, moreover, a sensitive intensity calibration for laser pulses that directly measures the maximum electric field strength in the material. Finally, the photogalvanic effect may also be investigated by associated terahertz emission [60–62].

Acknowledgments

This work was supported by the Austrian Science Fund (FWF): P21141-N16, special research programmes SFB-041 ViCoM, SFB-049 Next Lite and doctoral college W1243. GW thanks the IMPRS-APS for financial support. X-MT was supported by a Grant-in-Aid for Scientific Research (C24540421) from the JSPS. KY acknowledges support by the Grants-in-Aid for Scientific Research Nos. 23340113 and 25104702. Calculations were performed using the Vienna Scientific Cluster (VSC) and the supercomputer at the Institute of Solid State Physics, University of Tokyo.

References

[1] Krausz F and Ivanov M 2009 *Rev. Mod. Phys.* **81** 163
[2] Scrinzi A, Ivanov M Y, Kienberger R and Villeneuve D M 2006 *J. Phys. B: At. Mol. Opt. Phys.* **39** R1
[3] Cavalieri A L *et al* 2007 *Nature* **449** 1029
[4] Gertsvolf M, Jean-Ruel H, Rajeev P, Klug D, Rayner D and Corkum P 2008 *Phys. Rev. Lett.* **101** 243001
[5] Gertsvolf M, Spanner M, Rayner D M and Corkum P B 2010 *J. Phys. B: At. Mol. Opt. Phys.* **43** 131002
[6] Mitrofanov A V, Verhoef A J, Serebryannikov E E, Lumeau J, Glebov L, Zheltikov A M and Baltuška A 2011 *Phys. Rev. Lett.* **106** 147401
[7] Ghimire S, DiChiara A D, Sistrunk E, Agostini P, DiMauro L F and Reis D A 2011 *Nat. Phys.* **7** 138
[8] Schultze M *et al* 2013 *Nature* **493** 75
[9] Schultze M *et al* 2014 *Science* **346** 1348
[10] Schubert O *et al* 2014 *Nat. Photonics* **8** 119
[11] Lemell C, Tong X M, Krausz F and Burgdörfer J 2003 *Phys. Rev. Lett.* **90** 076403
[12] Dombi P *et al* 2004 *New J. Phys.* **6** 39
[13] Krüger M, Schenk M and Hommelhoff P 2011 *Nature* **475** 78
[14] Wachter G, Lemell C, Burgdörfer J, Schenk M, Krüger M and Hommelhoff P 2012 *Phys. Rev.* B **86** 035402
[15] Zherebtsov S *et al* 2011 *Nat. Phys.* **7** 656
[16] Neppl S *et al* 2015 *Nature* **517** 342
[17] Schiffrin A *et al* 2013 *Nature* **493** 70
[18] Paasch-Colberg T *et al* 2014 *Nat. Photonics* **8** 214
[19] Krausz F and Stockman M I 2014 *Nat. Photonics* **8** 205
[20] Ullrich C A, Gossmann U J and Gross E K U 1995 *Ber. Bunsenges. Phys. Chem.* **99** 488
[21] van Gisbergen S J A, Snijders J G and Baerends E J 1997 *Phys. Rev. Lett.* **78** 3097
[22] Calvayrac F, Reinhard P G, Suraud E and Ullrich C A 2000 *Phys. Rep.* **337** 493
[23] Takimoto Y, Vila F D and Rehr J J 2007 *J. Chem. Phys.* **127** 154114
[24] Akagi H, Otobe T, Staudte A, Shiner A, Turner F, Dörner R, Villeneuve D M and Corkum P B 2009 *Science* **325** 1364
[25] Otobe T 2012 *J. Appl. Phys.* **111** 093112
[26] Shinohara Y, Sato S A, Yabana K, Iwata J I, Otobe T and Bertsch G F 2012 *J. Chem. Phys.* **137** 224527
[27] Lee K M, Kim C M, Sato S A, Otobe T, Shinohara Y, Yabana K and Jeong T M 2014 *J. Appl. Phys.* **115** 053519
[28] Yabana K and Bertsch G F 1996 *Phys. Rev.* B **54** 4484
[29] Bertsch G F, Iwata J I, Rubio A and Yabana K 2000 *Phys. Rev.* B **62** 7998
[30] Onida G, Reining L and Rubio A 2002 *Rev. Mod. Phys.* **74** 601
[31] Marques M A L and Gross E K U 2004 *Ann. Rev. Phys. Chem.* **55** 427
[32] Otobe T, Yabana K and Iwata J I 2009 *J. Phys.: Condens. Matter* **21** 064224
[33] Wachter G, Lemell C, Burgdörfer J, Sato S A, Tong X M and Yabana K 2014 *Phys. Rev. Lett.* **113** 087401
[34] Troullier N and Martins J L 1991 *Phys. Rev.* B **43** 1993
[35] Tran F and Blaha P 2009 *Phys. Rev. Lett.* **102** 226401
[36] Koller D, Tran F and Blaha P 2011 *Phys. Rev.* B **83** 195134
[37] Koller D, Tran F and Blaha P 2012 *Phys. Rev.* B **85** 155109
[38] Berger J, de Boeij P and van Leeuwen R 2007 *Phys. Rev.* B **75** 035116
[39] Ruggenthaler M and Bauer D 2009 *Phys. Rev. Lett.* **102** 233001
[40] Fuks J I, Helbig N, Tokatly I V and Rubio A 2011 *Phys. Rev.* B **84** 075107
[41] Kurzweil Y and Baer R 2008 *Phys. Rev.* B **77** 085121
[42] Philipp H R 1966 *Solid State Commun.* **4** 73
[43] Yabana K, Sugiyama T, Shinohara Y, Otobe T and Bertsch G F 2012 *Phys. Rev.* B **85** 045134
[44] Resta R and Vanderbilt D 2007 *Theory of Polarization: A Modern Approach Physics of Ferroelectrics* (*Topics in Applied Physics no 105*) (Berlin: Springer) p 31
[45] Bernardi M, Vigil-Fowler D, Lischner J, Neaton J B and Louie S G 2014 *Phys. Rev. Lett.* **112** 257402
[46] Neuhauser D and Lopata K 2008 *J. Chem. Phys.* **129** 134106
[47] Glass A M, von der Linde D and Negran T J 1974 *Appl. Phys. Lett.* **25** 233
[48] Belinicher V I and Sturman B I 1980 *Usp. Fiz. Nauk* **130** 415

[49] Sturman P J and Fridkin V M 1992 *Photovoltaic and Photo-refractive Effects in Noncentrosymmetric Materials* (Boca Raton, FL: CRC Press)
[50] Fridkin V M 2001 *Crystallogr. Rep.* **46** 654
[51] Glazov M M and Ganichev S D 2014 *Phys. Rep.* **535** 101
[52] Alon O 2003 *Phys. Rev.* B **67** 121103 R
[53] Sipe J E and Shkrebtii A I 2000 *Phys. Rev.* B **61** 5337
[54] von Baltz R and Kraut W 1981 *Phys. Rev.* B **23** 5590
[55] Young S M, Zheng F and Rappe A M 2012 *Phys. Rev. Lett.* **109** 236601
[56] Nastos F and Sipe J E 2006 *Phys. Rev.* B **74** 035201
[57] Nastos F and Sipe J E 2010 *Phys. Rev.* B **82** 235204
[58] Perdew J P and Zunger A 1981 *Phys. Rev.* B **23** 5048
[59] Larochelle S F J, Talebpour A and Chin S L 1998 *J. Phys. B: At. Mol. Opt. Phys.* **31** 1215
[60] Gildenburg V B and Vvedenskii N V 2007 *Phys. Rev. Lett.* **98** 245002
[61] Sames C, Ménard J M, Betz M, Smirl A L and van Driel H M 2009 *Phys. Rev.* B **79** 045208
[62] Silaev A A and Vvedenskii N V 2009 *Phys. Rev. Lett.* **102** 115005